Electronic Supporting Information

Unravelling Structural Insights into Ligand-Induced Photoluminescence Mechanisms of Sulfur Dots

Satya Ranjan Sahoo[a,b], Arun Mukhopadhyay[a,b], Sukhendu Mahata[a,b], Komal Kumari[c], N. V. S. Praneeth[e], Ananya Baksi[d], Saumyakanti Khatua[e], Sumit Saha[a,b], Surajit Rakshit[c], and Nirmal Goswami*[a,b]

[a]Materials Chemistry Department, CSIR-Institute of Minerals and Materials Technology, Bhubaneswar 751013, Odisha, India

[b]Academy of Scientific and Innovative Research (AcSIR), Ghaziabad 201002, Uttar Pradesh, India.

[c]Department of Chemistry, Institute of Science, Banaras Hindu University, Varanasi 221005, Uttar Pradesh, India

[d]Department of Chemistry, Jadavpur University, Kolkata 700032, West Bengal, India

[e]Department of Chemistry, Indian Institute of Technology-Gandhinagar, Palaj 382355, Gujarat, India.

*Corresponding Author's Email: ngoswami@immt.res.in

TABLE OF CONTENT

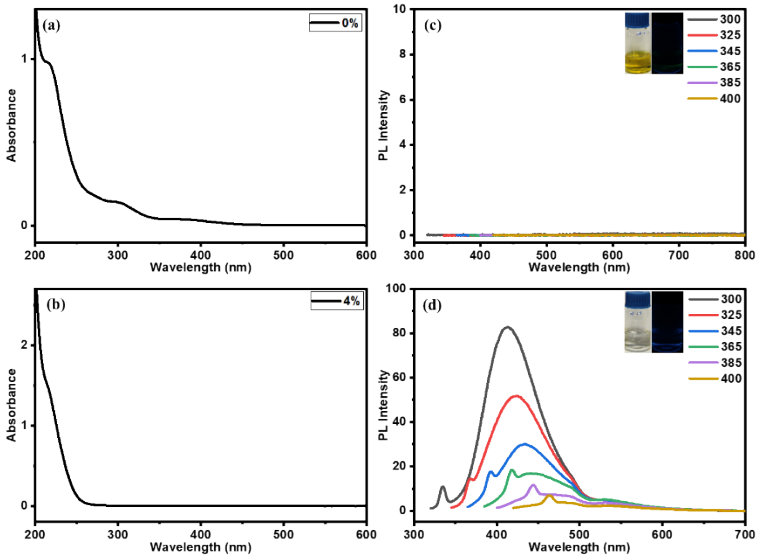

Figure S1. UV-vis spectra of **(a)** S-QD and **(b)** S-QD_4%. Excitation-dependent PL Spectra of **(c)** S-QD and **(d)** S-QD_4%. Inset: Photographs of S-QD and S-QD_4% respectively in visible and UV light (365 nm).

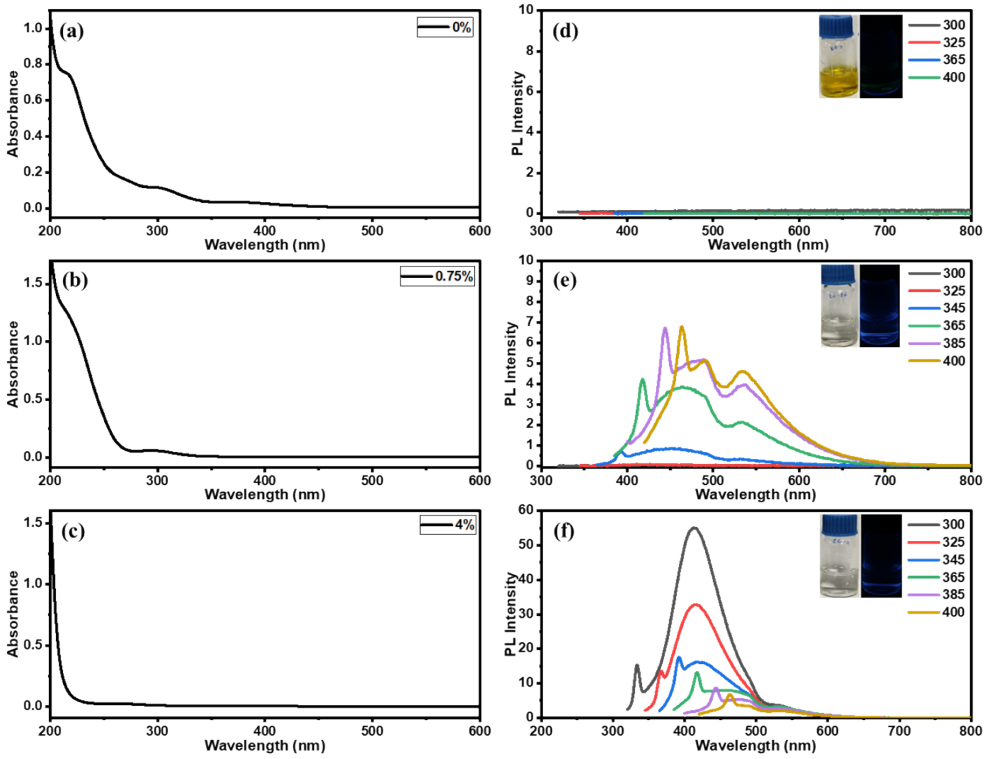

Figure S2. UV-vis spectra of (a) S-QD@EG, (b) S-QD@EG_0.75%, and (c) S-QD@EG_4%. Excitation-dependent PL Spectra of (d) S-QD@EG, (e) S-QD@EG_0.75%, and (f) S-QD@EG_4%. Inset: Photographs of S-QD@EG, S-QD@ EG_0.75%, and S-QD@ EG_4% respectively in visible and UV light (365 nm).

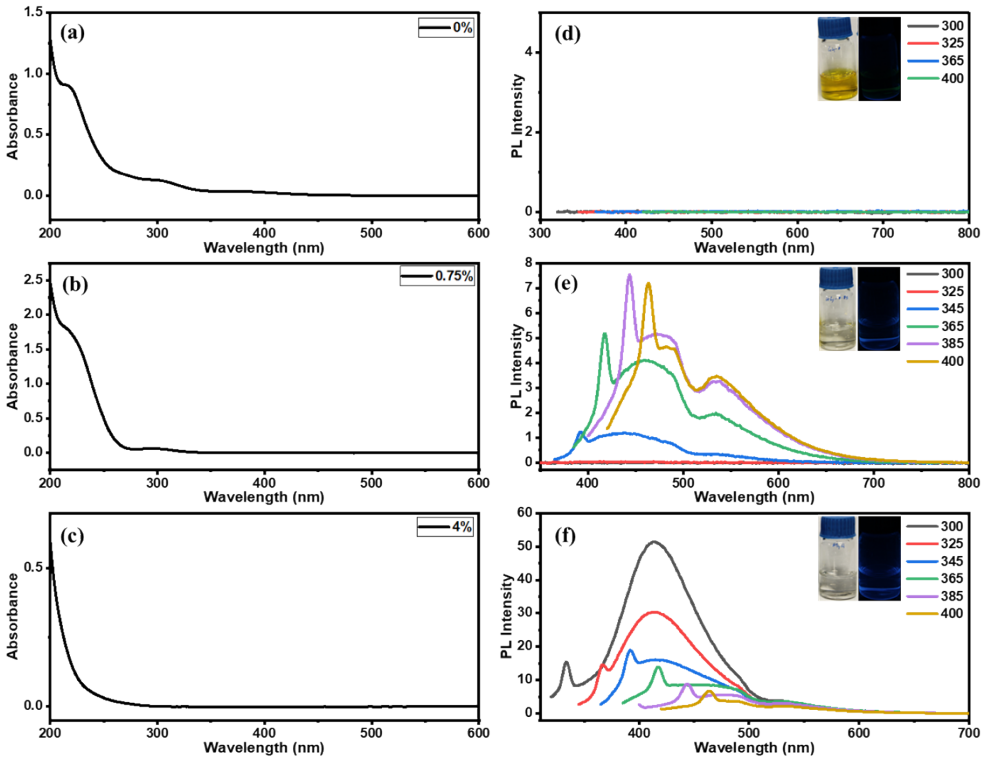

Figure S3. UV-vis spectra of **(a)** S-QD@Gly, **(b)** S-QD@Gly_0.75%, and **(c)** S-QD@Gly_4%. Excitation-dependent PL Spectra of **(d)** S-QD@Gly, **(e)** S-QD@Gly_0.75%, and **(f)** S-QD@Gly_4%. Inset: Photographs of S-QD@Gly, S-QD@Gly_0.75%, and S-QD@Gly_4% respectively in visible and UV light (365 nm).

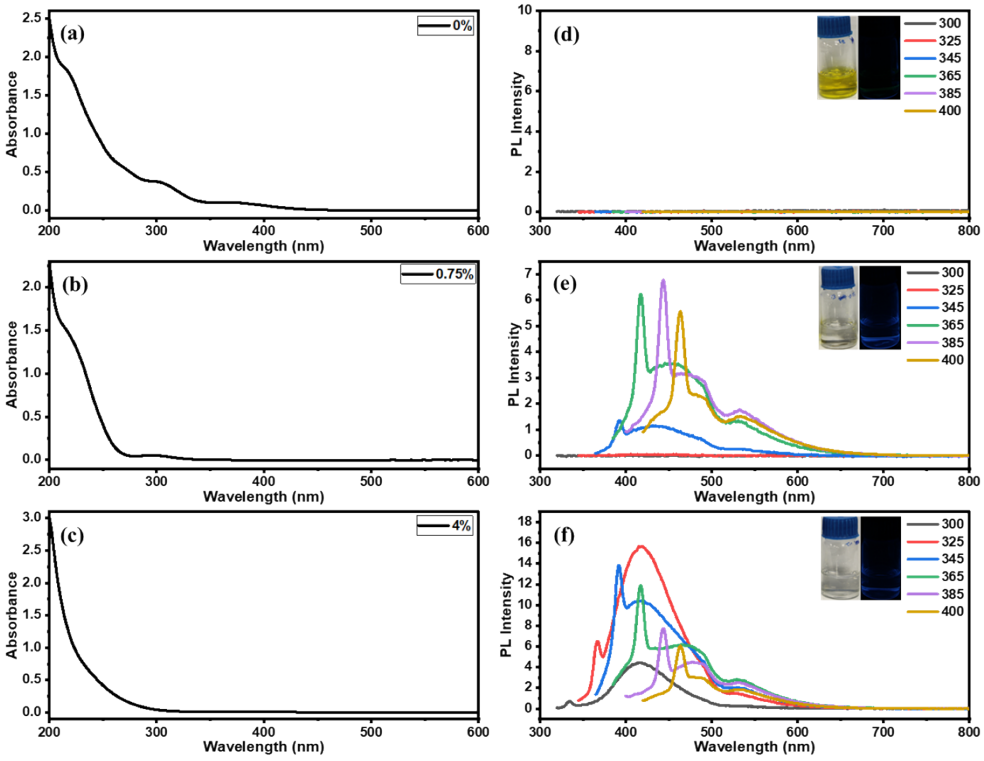

Figure S4. UV-vis spectra of **(a)** S-QD@TA, **(b)** S-QD@TA _0.75%, and **(c)** S-QD@TA _4%. Excitation-dependent PL Spectra of **(d)** S-QD@ TA, **(e)** S-QD@ TA _0.75%, and **(f)** S-QD@TA _4%. Inset:

Photographs of S-QD@TA, S-QD@TA _0.75%, and S-QD@TA _4% respectively in visible and UV light (365 nm).

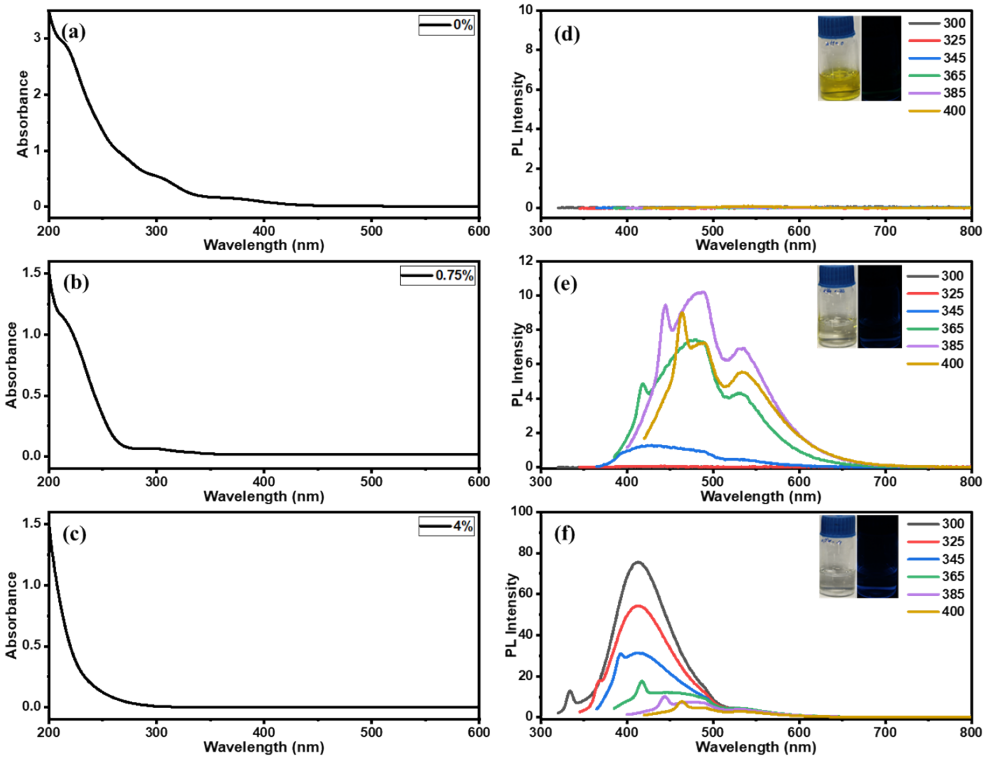

Figure S5. UV-vis spectra of **(a)** S-QD@MHA, **(b)** S-QD@MHA_0.75%, and **(c)** S-QD@MHA_4%. Excitation-dependent PL Spectra of **(d)** S-QD@MHA, **(e)** S-QD@MHA_0.75%, and **(f)** S-QD@MHA_4%. Inset: Photographs of S-QD@MHA, S-QD@MHA_0.75%, and S-QD@MHA_4% respectively in visible and UV light (365 nm).

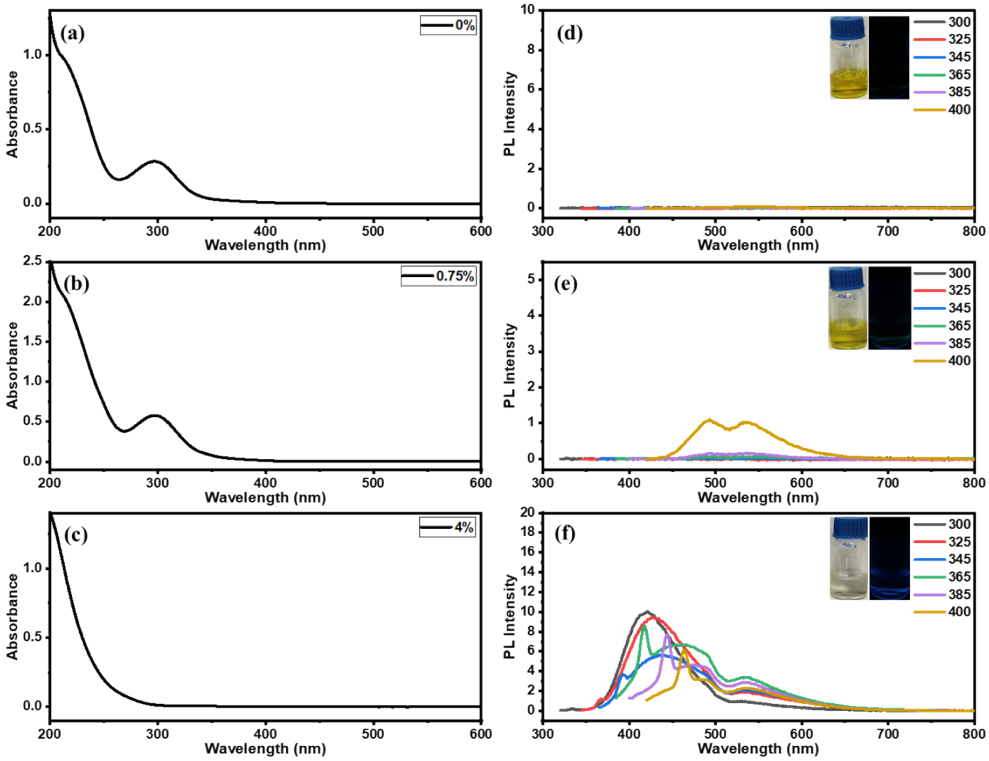

Figure S6. UV-vis spectra of **(a)** S-QD@MSA, **(b)** S-QD@MSA_0.75%, and **(c)** S-QD@MSA_4%. Excitation-dependent PL Spectra of **(d)** S-QD@MSA, **(e)** S-QD@MSA_0.75%, and **(f)** S-QD@MSA_4%. Inset: Photographs of S-QD@MSA, S-QD@MSA_0.75%, and S-QD@MSA_4% respectively in visible and UV light (365nm).

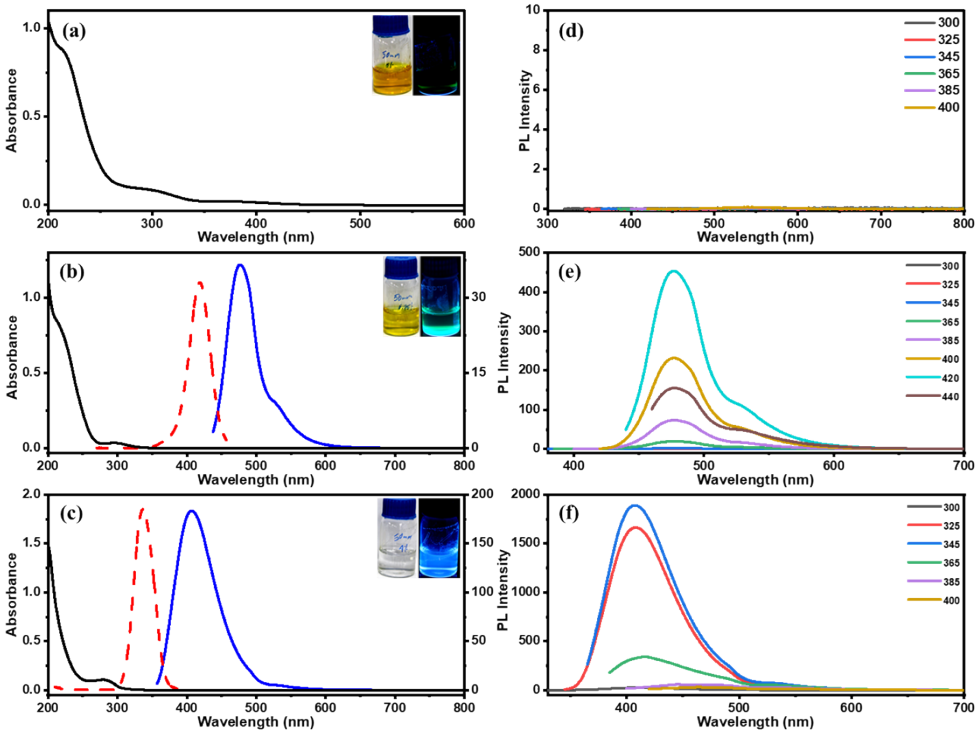

Figure S7. UV-vis (black solid line), PL emission spectra (blue solid line), and excitation spectra (red dash line) of **(a)** S-QD@GSH_0%, **(b)** S-QD@GSH_Green and **(c)** S-QD@GSH_Blue. Inset: Photographs of S-QD@GSH, S-QD@GSH_Green, and S-QD@GSH_Blue respectively in visible and UV light (365 nm). Excitation-dependent PL Spectra of **(d)** S-QD@GSH, **(e)** S-QD@GSH_0.75%, and **(f)** S-QD@GSH_4%.

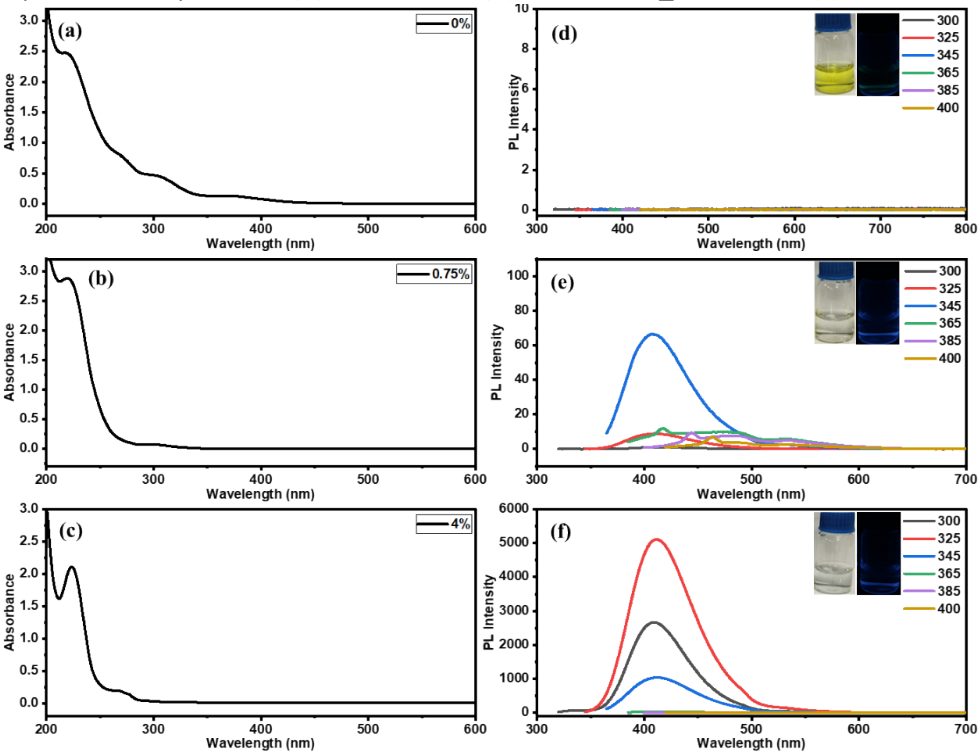

Figure S8. UV-vis spectra of **(a)** S-QD@BA, **(b)** S-QD@BA_0.75%, and **(c)** S-QD@BA_4%. Excitation-dependent PL Spectra of **(d)** S-QD@BA, **(e)** S-QD@BA_0.75%, and **(f)** S-QD@BA_4%. Inset: Photographs of S-QD@BA, S-QD@BA_0.75%, and S-QD@BA_4% respectively in visible and UV light (365 nm).

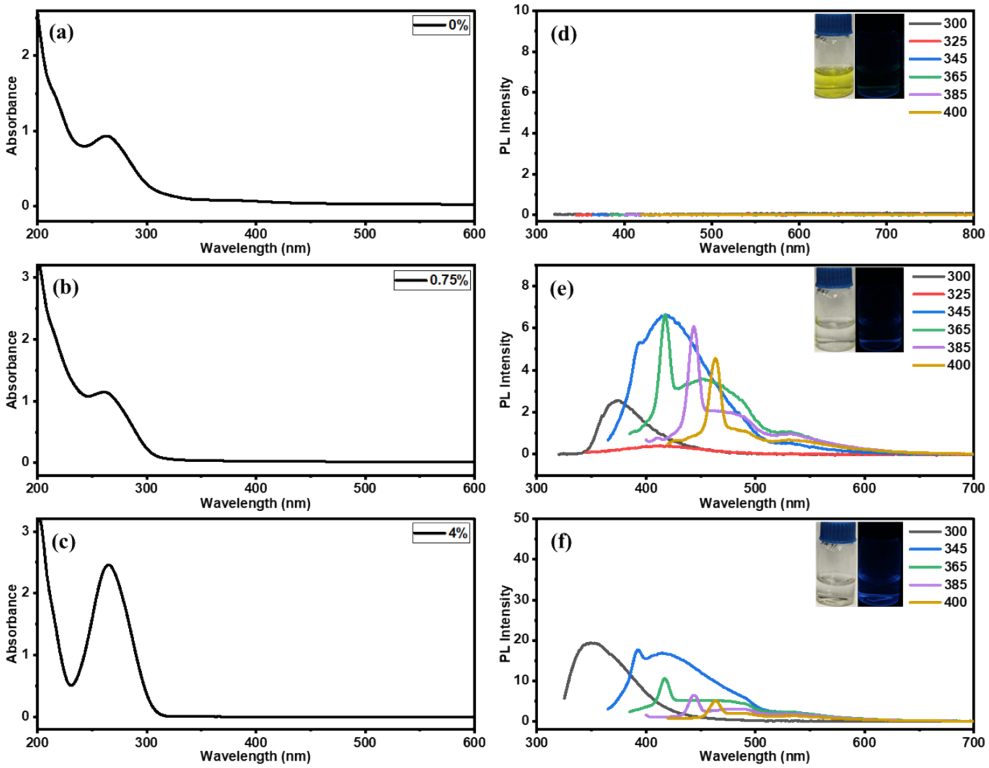

Figure S9. UV-vis spectra of **(a)** S-QD@ABA, **(b)** S-QD@ABA_0.75%, and **(c)** S-QD@ABA_4%. Excitation-dependent PL Spectra of **(d)** S-QD@ABA, **(e)** S-QD@ABA_0.75%, and **(f)** S-QD@ABA_4%. Inset: Photographs of S-QD@ABA, S-QD@ABA_0.75%, and S-QD@ABA_4% respectively in visible and UV light (365 nm).

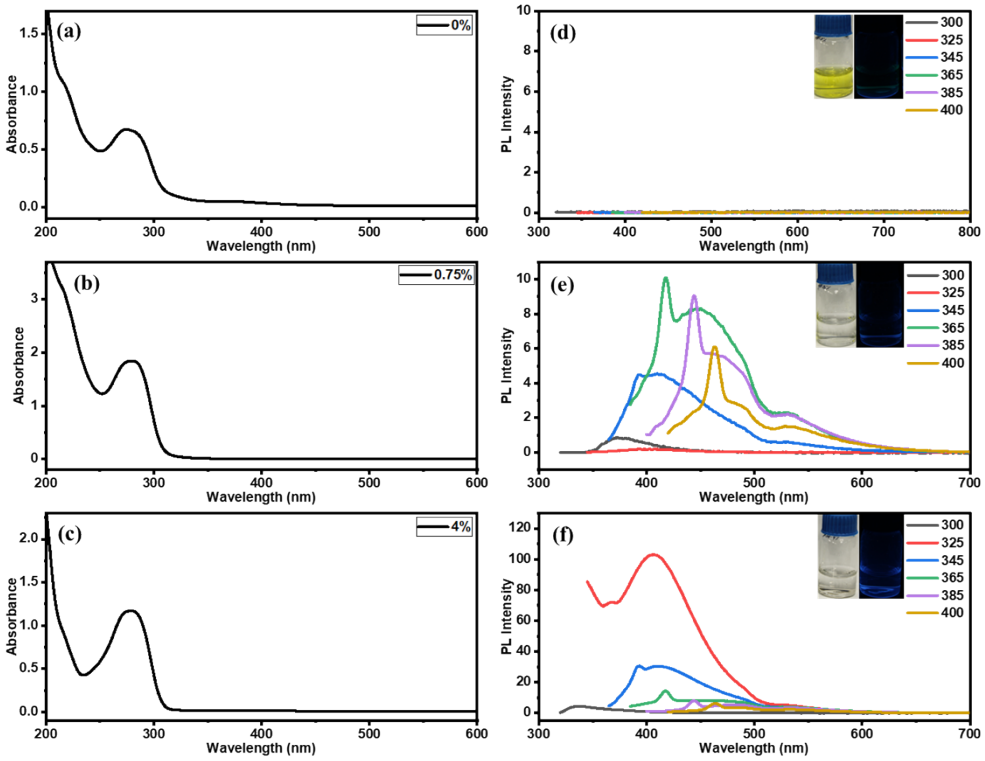

Figure S10. UV-vis spectra of **(a)** S-QD@HBA, **(b)** S-QD@HBA_0.75%, and **(c)** S-QD@HBA_4%. Excitation-dependent PL Spectra of **(d)** S-QD@HBA, **(e)** S-QD@HBA_0.75%, and **(f)** S-QD@HBA_4%. Inset: Photographs of S-QD@HBA, S-QD@HBA_0.75%, and S-QD@HBA_4% respectively in visible and UV light (365 nm).

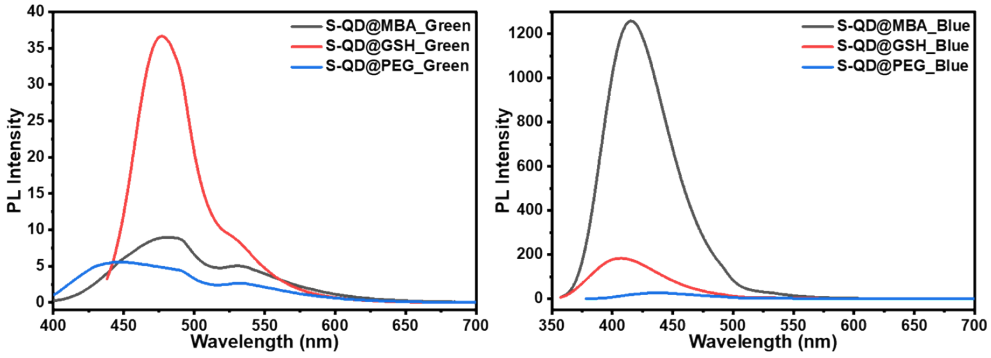

Figure S11. PL spectra of **(a)** S-QD@MBA_Green (grey line), S-QD@GSH_Green (red line), and S-QD@PEG_Green (blue line). **(b)** S-QD@MBA_Blue (grey line), S-QD@GSH_ Blue (red line), and S-QD@PEG_ Blue (blue line).

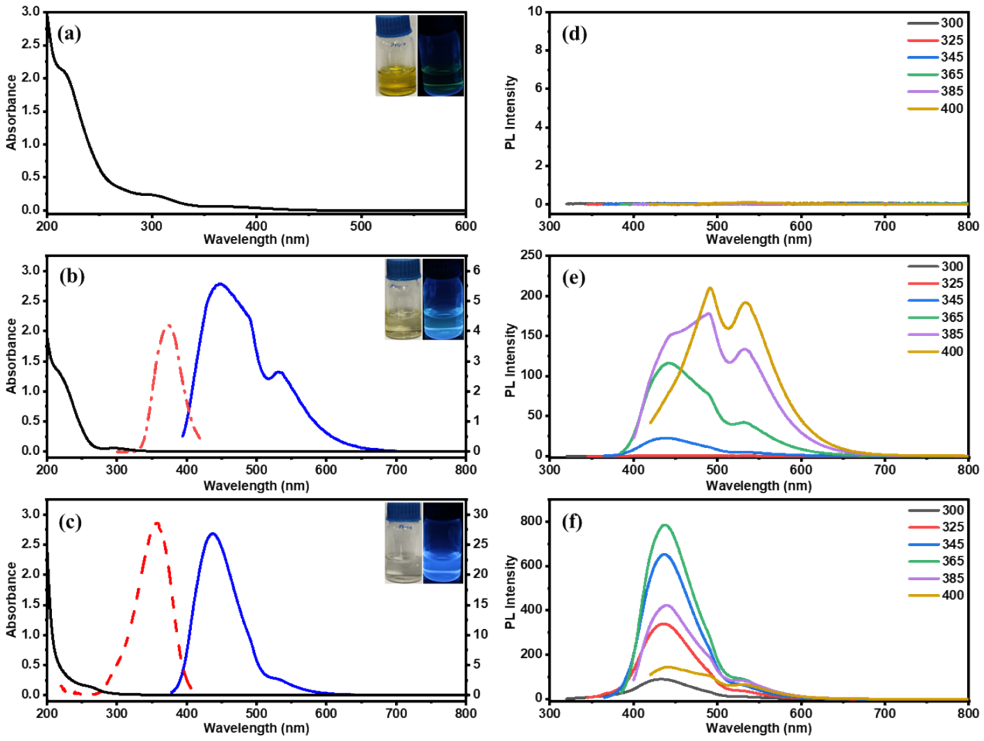

Figure S12. UV-vis (black solid line), PL emission spectra (blue solid line), and excitation spectra (red dash line) of **(a)** S-QD@PEG_0%, **(b)** S-QD@PEG_Green and **(c)** S-QD@PEG_Blue. Inset: Photographs of S-QD@PEG, S-QD@PEG_Green, and S-QD@PEG_Blue respectively in visible and UV light (365 nm). Excitation-dependent PL Spectra of **(d)** S-QD@PEG, **(e)** S-QD@PEG_0.75%, and **(f)** S-QD@PEG_4%.

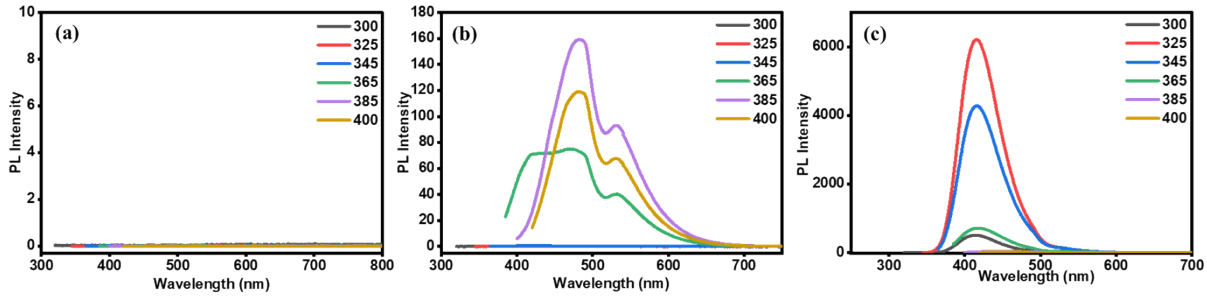

Figure S13. Excitation-dependent PL Spectra of **(a)** S-QD@MBA, **(b)** S-QD@MBA_Green, and **(c)** S-QD@MBA_Blue.

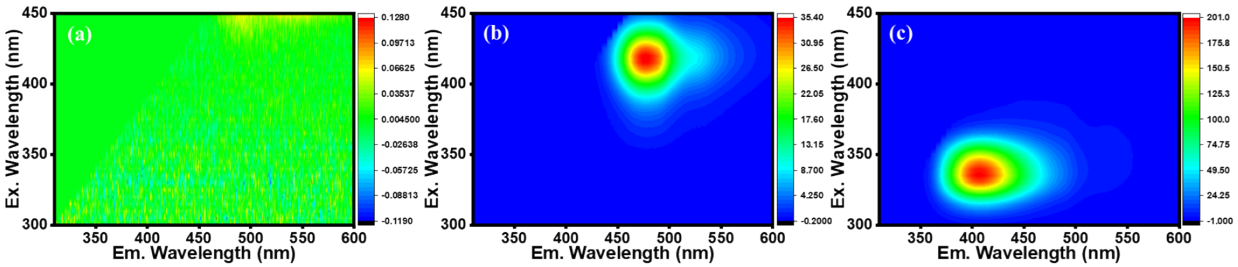

Figure S14. 3D PL excitation(y-axis) emission(x-axis) intensity spectra of **(a)** S-QD@GSH, **(b)** S-QD@GSH_Green, and **(c)** S-QD@GSH_Blue.

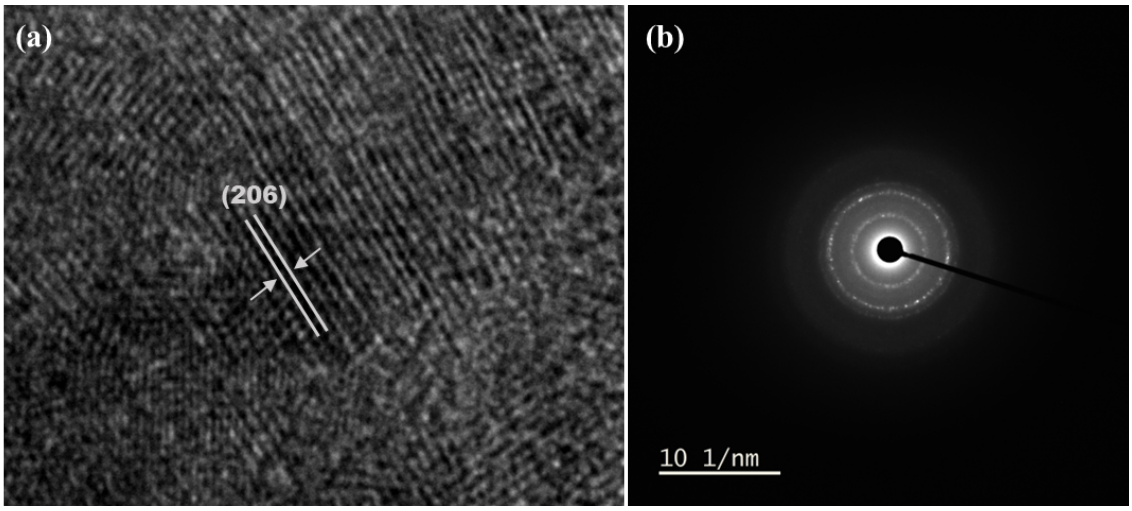

Figure S15. HRTEM image showing **(a)** d-spacing and **(b)** SAED pattern of S-QD@MBA_Blue.

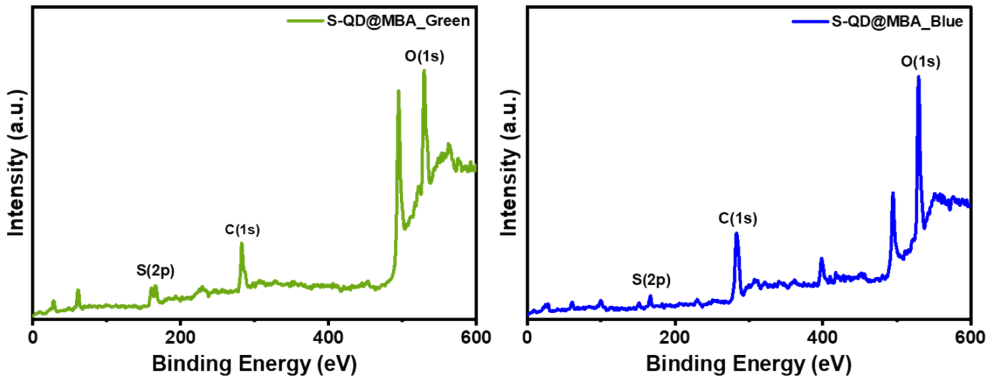

Figure S16. XPS Survey spectra of **(a)** S-QD@MBA_Green and **(b)** S-QD@MBA_Blue.

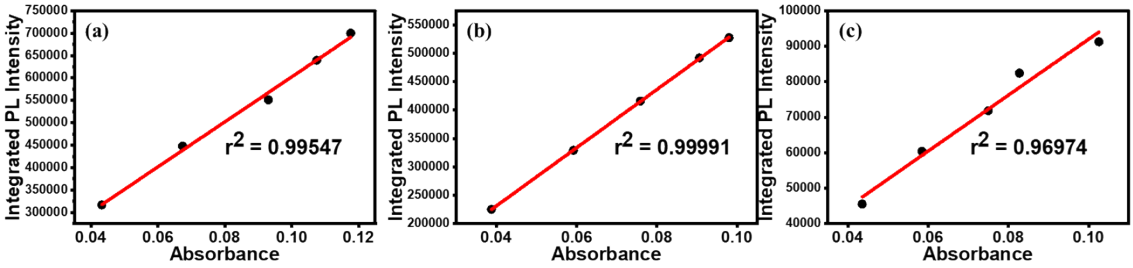

Figure S17. Plots of PL intensity of **(a)** Quinine (referenced dye), **(b)** S-QD@MBA_Blue, and **(c)** S-QD@GSH_Blue as a function of optical absorbance at 346 nm.

Table S1. PL QY calculation S-QD@MBA_Blue and S-QD@GSH_Blue.

Sample Name	Slope	PL QY (in %)
Quinine	5015334.154	55% (reported)
S-QD@MBA_Blue	5124959.139	56.2% (calculated)
S-QD@GSH_Blue	788519.1168	8.6% (calculated)

Table S2. PL lifetimes obtained from exponential fittings of experimental PL decays detected at different wavelengths for S-QD@MBA_Green and S-QD@MBA_Blue.

Sample Name	Wavelength (nm)	τ_1 (ns)	A_1	τ_2 (ns)	A_2	τ_{avg} (ns)
S-QD@MBA_Green	410	1.2141	0.557142857	10.0972	0.442857143	5.148044286
	450	1.1516	0.671232877	8.5558	0.328767123	3.585857534
	480	1.8208	0.617647059	7.4273	0.382352941	3.964461765
	530	2.5083	0.734375	7.131	0.265625	3.736204688
S-QD@MBA_Blue	410	1.0436	0.068965517	7.8284	0.931034483	7.360482759
	450	1.0756	0.086206897	7.6516	0.913793103	7.084703448
	480	1.6446	0.285714286	7.5408	0.714285714	5.856171429
	530	1.9029	0.833333333	7.5113	0.166666667	2.837633333

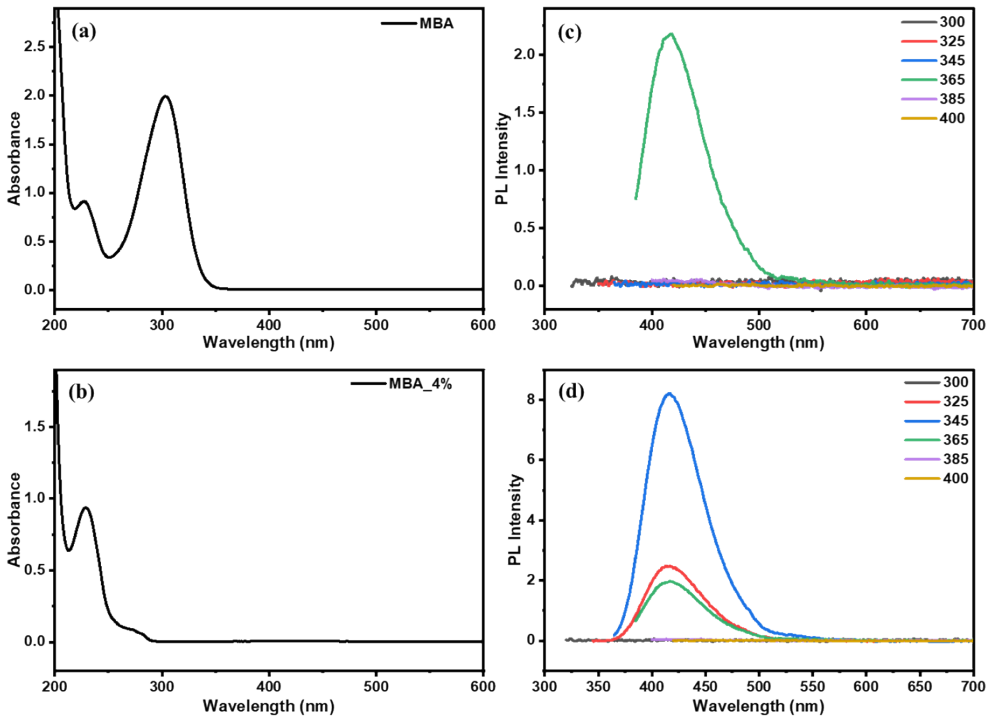

Figure S18. UV-vis spectra of **(a)** MBA and **(b)** MBA _4%. PL spectra of **(c)** MBA **(d)** MBA _4% at different excitation wavelengths.

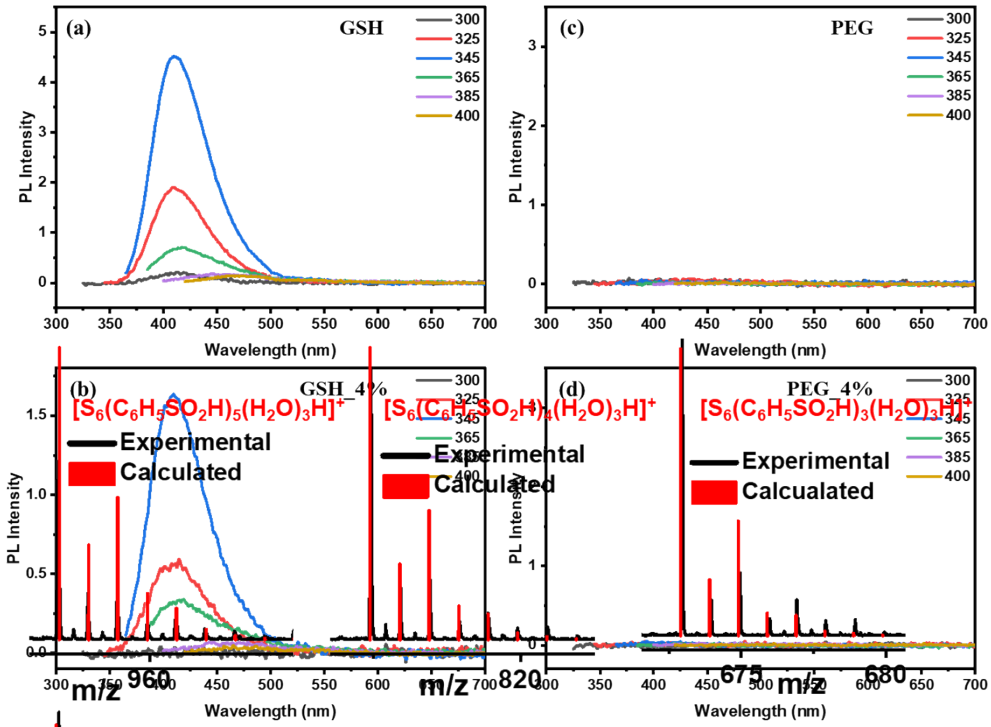

Figure S19. PL spectra of **(a)** GSH **(b)** GSH_4% **(c)** PEG (d) PEG_4% at different excitation wavelengths.

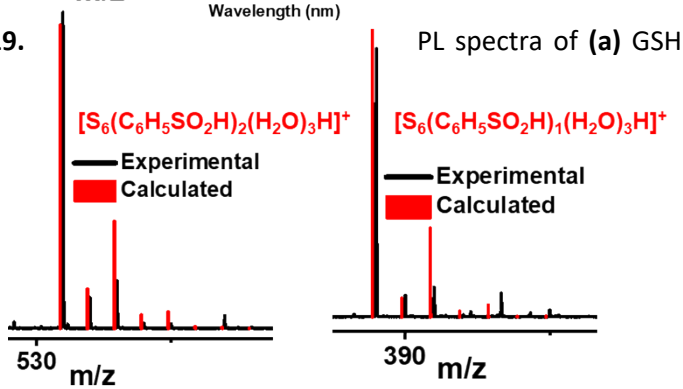

Figure S20. ESI MS of S_6 series compared with their theoretically calculated isotope patterns of respective species.

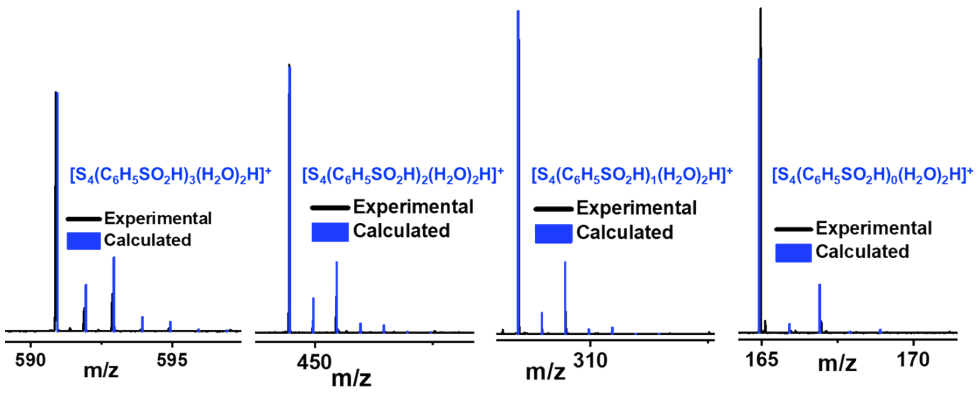

Figure S21. ESI MS of S_4 series compared with their theoretically calculated isotope patterns of respective species.

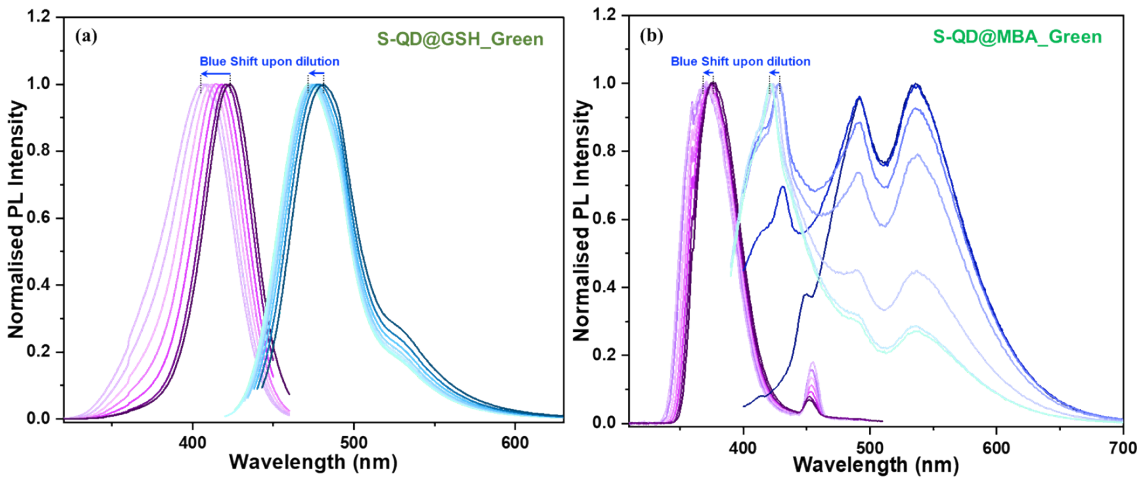

Figure S22. Concentration-dependent normalized PL excitation and emission spectra of **(a)** S-QD@GSH_Green and **(b)** S-QD@MBA_Green.

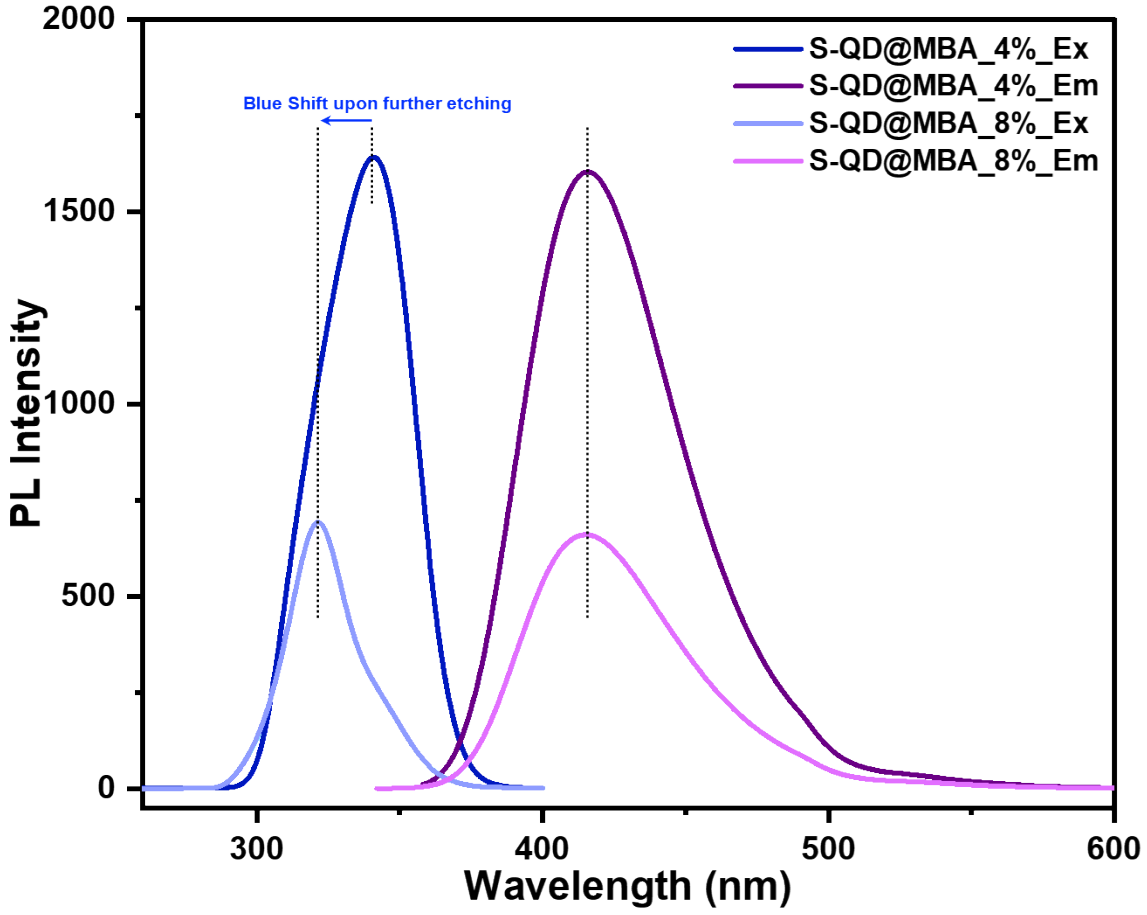

Figure S23. PL excitation and emission spectra of S-QD@MBA at 4% and 8% of H_2O_2 concentration.

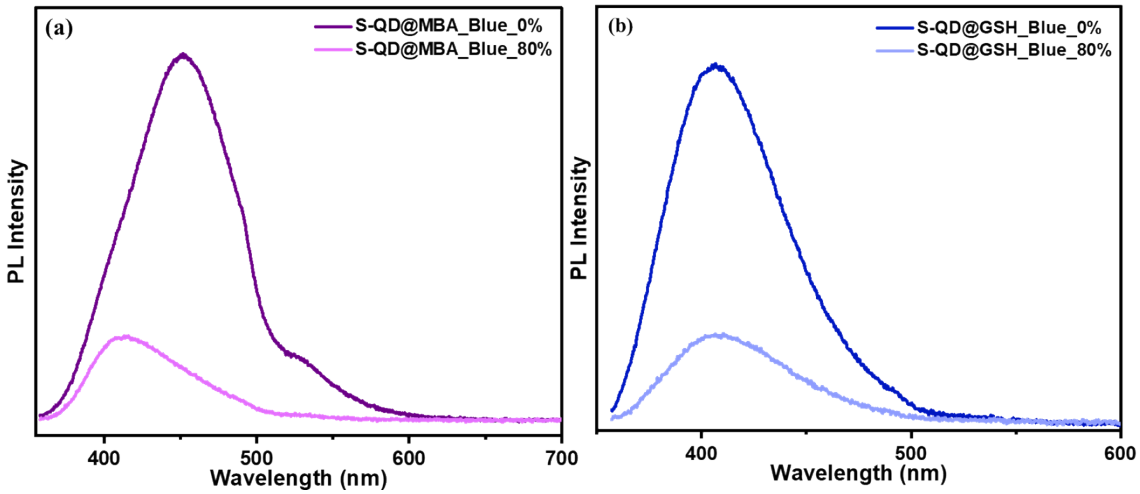

Figure S24. PL Spectra of **(a)** S-QD@MBA_Blue and **(b)** S-QD@GSH_Blue after treating with 80% ethanol.

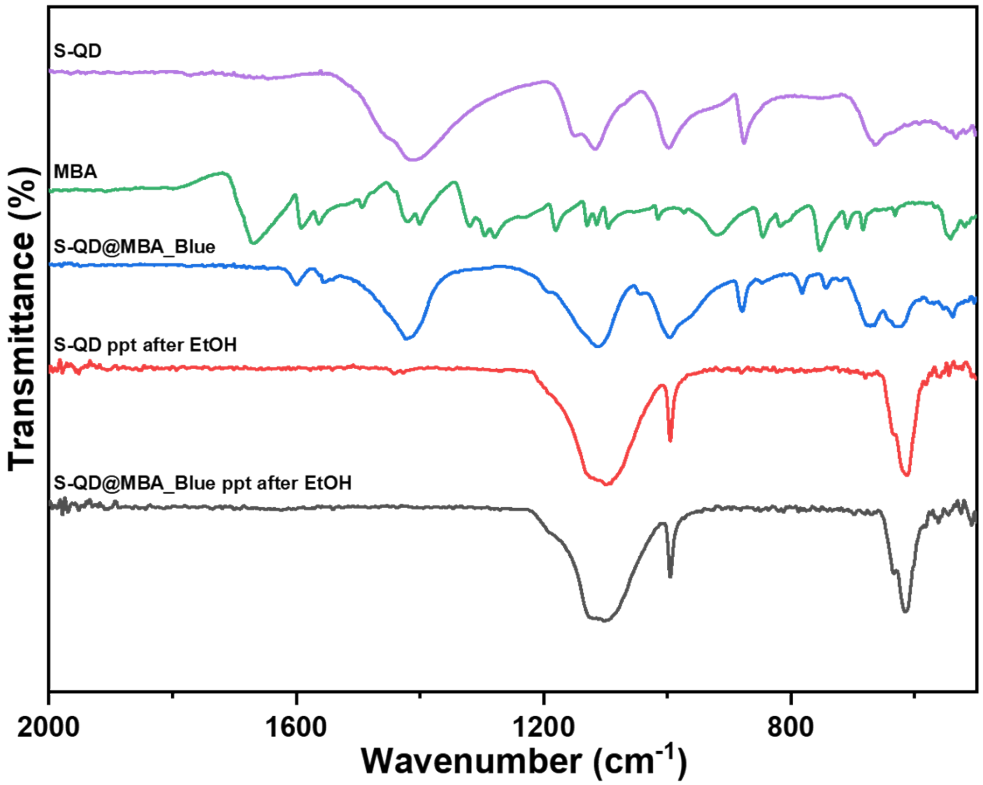

Figure S25. FTIR spectra of solid precipitate obtained after adding ethanol to S-QD@MBA_Blue (grey line), S-QD (red line) and compared with S-QD@MBA_Blue (Blue line), MBA ligand (green line) and S-QD (magenta line).

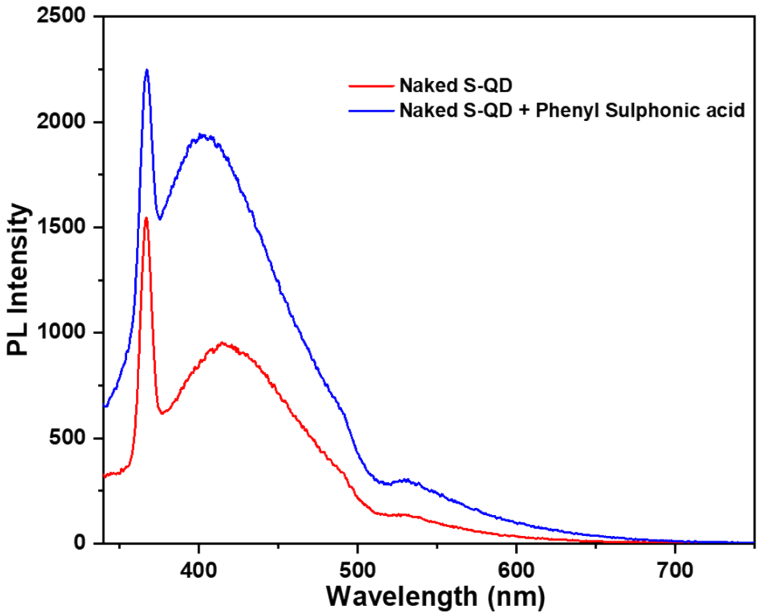

Figure S26. PL Spectra of Naked S-QD (red solid line) and naked S-QD + Phenyl Sulfonic Acid (50mM) (blue solid line).